Histochem Cell Biol (2011) 136:205–215
DOI 10.1007/s00418-011-0825-z

ORIGINAL PAPER

PTOV1 is associated with UCH-L1 and in response to estrogen stimuli during the mouse oocyte development

Yu-Wei Yao · Yan Shi · Zhe-Fu Jia · Ya-Hong Jiang · Zheng Gu · Jian Wang · Mohamad Aljofan · Zhao-Gui Sun

Accepted: 23 May 2011 / Published online: 16 June 2011

Abstract To investigate the biological significance of ubiquitin carboxyl-terminal hydrolase L1 (UCH-L1) involvement in oocyte maturation, we screened for proteins that bound to UCH-L1 in mouse ovaries, and we found that the prostate tumor overexpressed-1 (PTOV1) protein was able to bind to UCH-L1. PTOV1 is highly expressed in prostate cancers and considered as a potential marker for carcinogenesis and the progress of prostate cancer. It was reported that PTOV1 plays an important role in cell cycle regulation, but its role in mammalian oocyte development and meiosis is still unclear. In this paper, it was found that the expression levels of PTOV1 in mouse ovaries progressively increased from prepubescence to adulthood. And we found by immunohistochemistry that PTOV1 spreaded in both the cytoplasm and nuclei of oocytes during prepuberty, but in normal adult mouse oocytes, it concentrated not only in nuclei but also on the plasma membrane, though in some oocytes with abnormal shapes, PTOV1 did not display the typical distribution patterns. In granulosa cells, however, it was found to locate in the cytoplasm at all the selected ages. In postnatal mouse ovaries (28 days), estradiol treatment induced the adult-specific distribution pattern of PTOV1 in oocytes. In addition, UCH-L1 was shown to be associated with CDK1, which participated in the regulation of cell cycle and oocyte maturation. Therefore, we propose that the distribution changes of PTOV1 are age-dependent, and significant for mouse oocyte development and maturation. Moreover, the discovery that PTOV1 is associated with UCH-L1 in mouse oocytes supports the explanations for that UCH-L1 is involved in oocyte development and maturation, especially under the regulation of estrogen.

Keywords PTOV1 · UCH-L1 · Estradiol · Oocyte development

Abbreviations

PTOV1	Prostate tumor overexpressed-1
UCH-L1	Ubiquitin carboxyl-terminal hydrolase L1
GST	Glutathione S-transferase
CDK1	Cyclin-dependent kinase 1

Y.-W. Yao · Z.-F. Jia
Shanghai Medical College, Fudan University, Shanghai, China

Y.-W. Yao · Y. Shi · Z.-F. Jia · Y.-H. Jiang · Z. Gu · J. Wang · Z.-G. Sun (✉)
Key Laboratory of Contraceptive Drugs and Devices of National Population and Family Planning Committee, Shanghai Institute of Planned Parenthood Research, Shanghai, China
e-mail: sunzgbio@yahoo.cn

M. Aljofan
Prince Henry's Institute of Medical Research, Clayton, VIC 3168, Australia

Introduction

Oogenesis is a crucial event in sexual reproduction by which oocytes successively acquire their intrinsic abilities critical for fertilization and development of a healthy embryo (Hutt 2007; Sakai et al. 2004). Oogonia start the first meiotic division, and then oocyte stage begins in mouse embryos. Shortly after birth, meiosis in oocytes is arrested at the dictyate stage of late prophase in developing follicles. A small amount of the oocytes finally reach the ovulatory stage, and the fertile lifespan of a

female depends on the size of the oocyte pool at birth and its depletion speed with age (De Felici 2005; Miyano 2007). While granulosa cell contribution to oogenesis has been the focus in studies for many years, it has recently been suggested that the oocyte itself has a key role in determining its own fate (Plancha 2005; Sato et al. 2006; Song 2005). Estrogen promotes follicular development in which the actions of estrogen are culminated in ovulation by upregulating gonadotrophin receptors and gap junctions, and by inhibiting granulosa cell apoptosis (Rosenfeld et al. 2001).

Ubiquitin carboxyl-terminal hydrolase L1 (UCH-L1), formerly named as protein gene product 9.5 (PGP9.5), is named for its ubiquitin carboxyl-terminal hydrolase activity (Piccinini 1996; Wilkinson et al. 1986). UCH-L1 exists an oocyte-specific distribution and participates in the regulation of oocyte maturation in toads (Sun et al. 2002), and it contributes to the oocyte selective elimination in prepubertal mouse ovaries (Gu et al. 2009). To elucidate the functions of UCH-L1 in oocyte development and maturation, we used mass spectrographic technology to search for putative interaction partners of UCH-L1 and found that PTOV1 was a putative interacting protein. So, in the present paper we verified their association and focused on the possible contribution of PTOV1 in oocytes.

PTOV1 is first identified as a novel gene differentially expressed between prostate cancers and ambient normal tissues. The human *PTOV1* is located in chromosome 19q13.3, and it contains 12 exons and codes for a protein that consists of two novel homologous domains. These domains are arranged in tandem, without significant similarities to any known protein motifs, and they are conserved in humans, rodents and flies (Benedit et al. 2001). PTOV1 is overexpressed in prostate cancer cells (Benedit et al. 2001), and its protein expression is induced by testosterone (Nakamura et al. 2006). Recently, the expression level of PTOV1 is considered as a potential marker for the progression of prostate cancer (Morote et al. 2008).

Currently, the distribution of PTOV1 in mouse ovary is unknown. In this study, we demonstrated an association between UCH-L1, CDK1 and PTOV1 in mouse ovaries by GST-UCH-L1 pull-down combined with Western blotting and immunofluorescent colocalization assays. Then we demonstrated that subcellular localization of PTOV1 became gradually concentrated on the oocyte cytoplasmic membrane with age. A similar change of its distribution pattern was found in prepubertal mouse ovaries after estradiol administration, which suggested that estrogen profoundly affected the distribution of PTOV1 in mouse oocytes during prepubertal development.

Materials and methods

Animals and tissues

ICR female and male adult mice (56 days postnatal) were obtained from the Sino-British Sippr/BK Lab Animal Ltd, Shanghai, China. All the mice were raised in a controlled environment, with a temperature range between 22 to 24°C and a 14-h light and 10-h dark photoperiod. The mice were mated to get the offsprings. For the study about the expressional changes of UCH-L1 and PTOV1 with age, female mice aged 7 days (10 mice, 7 days postnatal), 14 days (10 mice, 14 days postnatal), 21 days (10 mice, 21 days postnatal), 28 days (10 mice, 28 days postnatal) and 56 days (10 mice, 56 days postnatal) were killed by cervical vertebrae luxation to collect the ovaries.

To study estrogen actions on prepubertal mouse ovaries, 10 mice (23 days) were divided into an experimental group (5 mice) and control group (5 mice). Mice in the experimental group administrated by intraperitoneal injection with estradiol (a main type of estrogen, Shanghai Tongyong Drug Ltd. Inc., Shanghai, China) at a dose of 7.5 μg/g body weight once a day at 9:00 am for five consecutive days, and mice in the control group were injected with corn oil. The estradiol administration was performed according to the previous experiments. On the sixth day (28 days), mice were killed by cervical vertebrae luxation. The experiments were repeated in triplicate.

All the experiments were in full compliance with standard laboratory animal care protocols approved by the Institutional Animal Care Committee of Shanghai Institute of Planned Parenthood Research.

Various tissue samples from ICR mice were collected, frozen in liquid nitrogen and stored at −80°C for western blot analysis; or fixed for paraffin sections; or frozen in a Trizol reagent (Invitrogen, Carlsbad, CA, USA) and stored at −80°C for Real time-PCR analysis.

Antibodies

Rabbit antisera were generated against the synthetic peptide WQEPRPEPNSRSKR, corresponding to residue 266–279 of mouse PTOV1, conjugated to KLH (keyhole limpet hemocyanin), and then the polyclonal antibody was purified from a total amount of IgG by antigen affinity chromatography. A certain amount of the rabbit antibody was labeled with fluorescein isothiocyanate (FITC) for the immunofluorescent reaction assay. The following antibodies were purchased: rabbit anti-p34^{cdc2} (also known as CDK1) (ABR Affinity BioReagents, CO, USA); rabbit anti-GAPDH, biotin-conjugated donkey-anti-rabbit IgG and HRP-streptavidin (Proteintech Group Inc., Chicago, IL, USA); rabbit anti-UCH-L1 and alkaline phosphatase-

conjugated goat anti-rabbit IgG (H + L) (Zymed, Laboratories Inc., USA); rabbit anti-beta-actin (Cell Signaling Technology, Ltd. Inc., USA); and Alexa Fluor 568 donkey-anti-rabbit IgG (H + L) (Invitrogen, Molecular Probes, USA).

Cell culture and RNA interference for testifying the specificity of the PTOV1 antibody

Human A549 cells (The Cell Bank of Type Culture Collection of Chinese Academy of Sciences) were cultured in RPMI1640 (Hyclone) supplemented with 10% fetal bovine serum (FBS) (Biowest), 50 μg/ml of streptomycin, 100 U/ml of penicillin and 2 mM glutamine.

The PTOV1-siRNA and a non-specific control were purchased from Santa Cruz Biotechnology and Invitrogen separately. siRNA duplex was transfected into human A549 cells with Lipofectamine 2000 transfection reagent (Invitrogen) as recommended by the manufacturer's instructions. The cells were harvested 24 and 48 h after transfection, separately. Then cells were lysed by lysis buffer (Beyotime Biotech Ltd, China), separated in 12% SDS-PAGE and detected by western blot analysis.

RNA extraction and RT-PCR

Trizol reagent (Invitrogen, Life Technologies Ltd, Renfrew, Strathclyde, UK) was used to isolate total RNA from pooled ovaries of five mice according to the manufacturer's protocol. Ovarian mRNA was subjected to RT with Quant Reverse Transcriptase (TianGen Biotech, Beijing, China). The primers used in RT-PCR analysis were as follows: UCH-L1, forward 5′-GAT TAA CCC CGA GAT GCT GA-3′ and reverse 5′-CCG ATG GTA CCA CAG GAG TT-3′; PTOV1, forward 5′-GTG GCA GGA GAA GCG TAG AC-3′ and reverse 5′-GCT GAG AGT TTC GGA ACA GG-3′; and beta-actin, forward 5′-AGC CAT GTA CGT AGC CAT CC-3′ and reverse 5′-CCG ATG GTA CCA CAG GAG TT-3′. PCR was then performed with Taq Master Mix (TianGen Biotech), cDNA templates (total RNA; 500 ng) and a loading buffer at the following cycling conditions for 34 cycles: 94°C for 30 s, 60°C for 30 s and 72°C for 30 s. The PCR products were authenticated by sequencing, and analyzed on a 2% agarose gel and stained with goldview (SBS Genetech, Beijing, China). Signals were photographed by a BioSens Gel Imaging System (Shanghai Bio-Tech, Shanghai, China). Changes in mRNA expression levels were calculated in reference to beta-actin.

Real time-PCR was performed with SYBR Green Real time PCR Master Mix (QPK-201, Toyobo Co., Ltd., Osaka, Japan) instead of general Taq Master Mix at the following cycling conditions for 40 cycles: 95°C for 15 s, 60°C for 15 s and 72°C for 45 s. The original mRNA copies were evaluated by $2^{-\Delta\Delta C_T}$ method (Livak and Schmittgen 2001), and the relative values to beta-actin were calculated for SPSS analysis.

Western blot analysis

Ovarian tissue protein extracts were obtained in the following ice-cold protein extraction buffer (EB): 50 mmol/L Hepes (pH 7.5) (Sigma, St. Louis, MO, USA), 100 mmol/L NaCl (Sigma), 10 mmol/L $MgCl_2$, 25 mmol/L β-glycerophosphate (Merck, Germany), 50 mmol/L NaF, 1 mmol/L EDTA, 1% Triton-100 (Sigma), 10 mg/ml soybean trypsin inhibitor (Sigma), 5 mg/ml leupeptin, 10 mg/ml aprotinin (Sigma), 100 mM Phenylmethanesulfonyl fluoride (PMSF) (Sigma) and 1 mM Na_3VO_4 (Sigma). The protein concentration of each total protein extract was determined by the Bradford assay. Western blot (WB) analysis was carried out as previously described (Sun et al. 2002). The proteins were detected with the following antibodies: rabbit anti-PTOV1 (1:500 dilution), rabbit anti-$p34^{cdc2}$ (1:1,000 dilution) and rabbit anti-UCH-L1 (1:200 dilution). The immunoreactive complexes on the membrane were visualized by staining for 3 min with a PhosphaGLO™ AP Substrate kit (KPL, Gaithersburg, MD, USA) according to the manufacturer's protocol. Beta-actin and GAPDH were used as sample loading controls with a rabbit polyclonal antibody (rabbit anti-beta-actin 1:1,000 dilution, and rabbit anti-GAPDH 1:1,000).

Pull-down assay and mass spectrographic technology

Ovarian protein extracts (1 mg of total protein) from 56-day-old mice were pre-absorbed with 100 μl of Sepharose Cl-6B (Amersham Pharmacia Biotech, NJ, USA), which was prewashed with cold PBS (pH 7.4), and the protein extracts were then mixed with 100 μl of Glutathione Sepharose 4B beads (Amersham Pharmacia Biotech, NJ, USA) coupled with glutathione S-transferase (GST beads). The supernatant was then incubated with Glutathione Sepharose 4B beads (Amersham Pharmacia Biotech, NJ, USA) coupled with GST-UCH-L1 fusion protein (GST-UCH-L1 beads) (Sun et al. 2003). The two types of beads (GST beads and GST-UCH-L1 beads) were washed and eluted with 50 μl of reduced glutathione elution buffer. The elution was collected and digested by trypsin enzymatic hydrolysis to form peptide fragments, then applied to the mass spectrometer (LTQ-Orbitrap, Thermo Finnigan, San Jose, CA, USA) to identify proteins contained (Proteome Research Center, Shanghai Institute of Biochemistry and Cell Biology, Chinese Academy of Sciences). Briefly, an in-house nano-electrospray source and an HP1100 solvent delivery system (Agilent

Technologies, CA, USA) were coupled to LTQ. Samples were automatically delivered by a FAMOS autosampler (LC Packings, San Francisco, CA, USA) to a 100-μm-internal diameter fused silica capillary precolumn packed with 2 cm of 200-Å pore size Magic C18AQ^{TM} material (Michrom Bioresources, Auburn, CA, USA). The samples were washed with solvent A (5% acetonitrile in 0.1% formic acid) on the precolumn, eluted with a gradient of 10–35% solvent B (100% acetonitrile) over 30 min to a 75-μm × 10-cm fused silica capillary column packed with 100-Å pore size Magic C18AQ material (Muchrom Bioresources), and then injected into the mass spectrometer at a constant column tip flow rate of ~300 nl/min. Eluting peptides were analyzed by nano-LC-MS acquisition.

Confirmation of the association of UCH-L1 and PTOV1

The two types of beads from the pull-down assay were washed four times in phosphate-buffered saline with Tween-20 (0.05% V/V), pH7.4 (PBST). The beads were then suspended in SDS-PAGE loading buffer (1×) for SDS-PAGE and western blot analysis.

Immunohistochemical characterization

Mouse ovaries were directly fixed in Bouin's fixative for 40 h. The ovaries were then dehydrated in graded alcohol and embedded in paraffin (Beijing Chemical, Beijing, China). Sections (5 μm) of ovarian tissues were processed for immunohistochemical detection with a rabbit anti-PTOV1 antibody (1:50 dilution) and were visualized by AEC (Liquid AEC-Plus Substrate kit, Boster Biological Technology, China) according to the manufacturer's protocol. For negative controls, 10% donkey serum was used instead of primary antibodies. The degree of staining was subjectively assessed by blind examination of the slides by three investigators independently. All the sections were examined and photographed under the microscope (DFC420C, Leica, Germany).

Immunofluorescent colocalization

Sections were incubated with rabbit anti-UCH-L1 (1:200 dilution) and Alexa Fluor 568 donkey-anti-rabbit IgG (H + L) (2 μg/μl) antibodies for general immunofluorescent staining. Other serial sections were stained with the FITC-conjugated rabbit anti-PTOV1 antibody (1:10 dilution). The sections were then examined under a fluorescent microscope (Nikon 50i, Japan), and pictures of the red and green fluorescence in serial sections were overlapped by Photoshop 7.0 (Adobe Systems Incorporated) to compare the localization of UCH-L1 and PTOV1.

Statistical analysis

The Tanon Gis program (Shanghai Bio-Tech) was used to evaluate the RNA and protein band intensity. The relative quantitative values of RNA and protein bands were obtained with reference to beta-actin. All data were analyzed using the SPSS13.0 software (SPSS Inc., Chicago, IL, USA). The differences between the estradiol-treated group and the control group were tested for significance using the independent sample t test. Statistical significance was defined as $p < 0.05$.

Results

PTOV1 is specifically bound to UCH-L1 in ovarian protein extracts

To investigate the potential functions of UCH-L1 in oocyte development and maturation, we screened for putative interacting proteins of UCH-L1. The proteins separated by the pull-down assay with the recombinant GST-UCH-L1 fusion protein from adult mouse ovarian protein extracts were identified by mass spectrographic technology. Comparing the pull-down of GST-UCH-L1 with GST, PTOV1 was identified to be included in the proteins isolated by UCH-L1 affinity. Western blot analysis was employed to confirm the association between UCH-L1 and PTOV1. GST-UCH-L1 pulled out a protein of 58 kDa molecular weight, which was recognized by PTOV1 antibody, from ovarian protein extracts of 56 days old mice, whereas the GST control did not (Fig. 1a). It has been reported that UCH-L1 binds to CDK1 in toad oocyte protein extracts (Sun et al. 2002), so we examined the protein-protein interaction of UCH-L1 and CDK1, and found that UCH-L1 was able to bind to CDK1 in mouse ovarian protein extracts (Fig. 1a).

Immunofluorescent colocalization of UCH-L1 and PTOV1 in mouse ovaries

We next examined whether the association between UCH-L1 and PTOV1 was present in ovarian tissues by their colocalization using double immunofluorescent staining. Immunofluorescence showed that UCH-L1 was exclusively localized in oocytes, but PTOV1 was localized in both oocytes and granulosa cells. Furthermore, the positive signals of both UCH-L1 and PTOV1 concentrated in oocyte nuclei and cytoplasm in similar spatial patterns in prepubertal mouse ovaries and were intensified at oocyte plasma membranes in adult mouse ovaries (Fig. 1b).

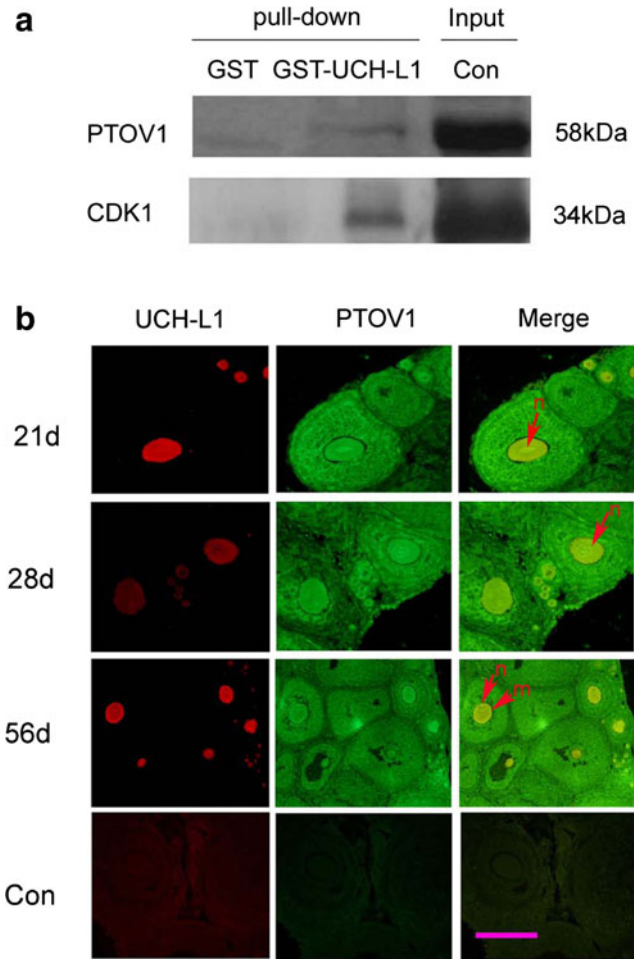

Fig. 1 Analysis of UCH-L1 and PTOV1 association in mouse ovaries. **a** UCH-L1 binds to PTOV1 and $p34^{cdc2}$ (or CDK1) from protein extracts of 56-day-old mouse ovaries. The ovarian protein extract was pulled down by Glutathione Sepharose 4B beads coupled with either GST or GST-UCH-L1, and the bound proteins were detected by western blot analysis for PTOV1 and $p34^{cdc2}$. The total protein extract (160 μg) was used as a control (Con). **b** Colocalization of UCH-L1 (*red*) and PTOV1 (*green*) by immunofluorescent staining in mouse ovaries. *Red arrows* indicate colocalization of UCH-L1 and PTOV1 staining at the plasma membrane (*m*) and in nuclei (*n*) of oocytes from mice at different ages (postnatal *21d*, *28d* and *56d*). The control (*Con*) are ovarian sections of postnatal (*56d*) mice processed in parallel but with removal of the primary antibody. *Pink bar* in the last panel marks 100 μm

PTOV1 and UCH-L1 expression and localization in various tissues of adult mice

The specificity of PTOV1 antibody was testified in lysates from human A549 cells which were tranfected with siRNA against *PTOV1*, and with scrambled siRNA as control. PTOV1 showed a specific band of 58 kDa in the control panel, but no band was detected in lysates from A549 cells tranfected with siRNA to interfere PTOV1 mRNA for 24 or 48 h (Fig. 2a).

As presented in Fig. 1, both PTOV1 and UCH-L1 were expressed in mouse ovaries, but it is worth to determine whether their expression and cellular distribution patterns are specific for ovarian tissues. So we checked the expression in other selected tissues of adult mouse as shown in Fig. 2b. High expression levels of UCH-L1 were detected in the mouse brain, ovary and testis, but no positive signal for UCH-L1 was found in the mouse skeletal muscle, kidney, uterus and heart. PTOV1 was most abundant in the ovary, uterus and heart, but it was expressed at low levels in the testis, skeletal muscle and kidney. Notably, PTOV1 was undetectable in the brain.

To further explore the cellular localization of PTOV1 in various adult mouse tissues, immunohistochemistry was performed. PTOV1 was detected in the cytoplasm of somatic cells from almost all the selected mouse tissues including oviduct epithelial mucosa cells, uterine endometrial epithelial cells, testicular elongating sperm cells and mature sperms, renal tubule epithelial cells, myocardial cells, skeletal muscle cells, lung epithelial cells, hepatocytes (Fig. 2c) and ovarian granulosa cells (Fig. 3c). No positive signals were found in the nuclei of these somatic cells, which was not the case in oocytes (Fig. 2c).

Protein and mRNA levels of PTOV1 and UCH-L1 in developing mouse ovaries

Western blot analysis indicated that the antibodies against PTOV1 or UCH-L1 recognized a specific single band in the protein extracts of mouse ovaries at different ages (Fig. 3a). Protein levels of PTOV1 in mouse ovaries increased with age from prepuberty to sexual maturity, and the increase was more obvious from postnatal day 7 to day 14 (Fig. 3b). A similar general trend was observed for UCH-L1 protein levels among different ages (Fig. 3b). However, the change of their corresponding mRNA levels with age did not show a similar rising tendency according to results by real time RT-PCR detection (Fig. 3c, d).

Localization of PTOV1 in mouse ovaries at different ages

In ovarian follicles from 1- to 4-week-old mice (7, 14, 21 and 28 days postnatal), immunohistochemical staining revealed that PTOV1 was present in both oocytes and granulosa cells at every follicular stage, which was determined according to the reported method (Bristol-Gould et al. 2006). In primodial follicles, it mainly existed in granulosa cells, and in primary follicles it was present in both granulosa cells and oocytes. It was noteworthy that, in some primary follicles, it was highly expressed both in

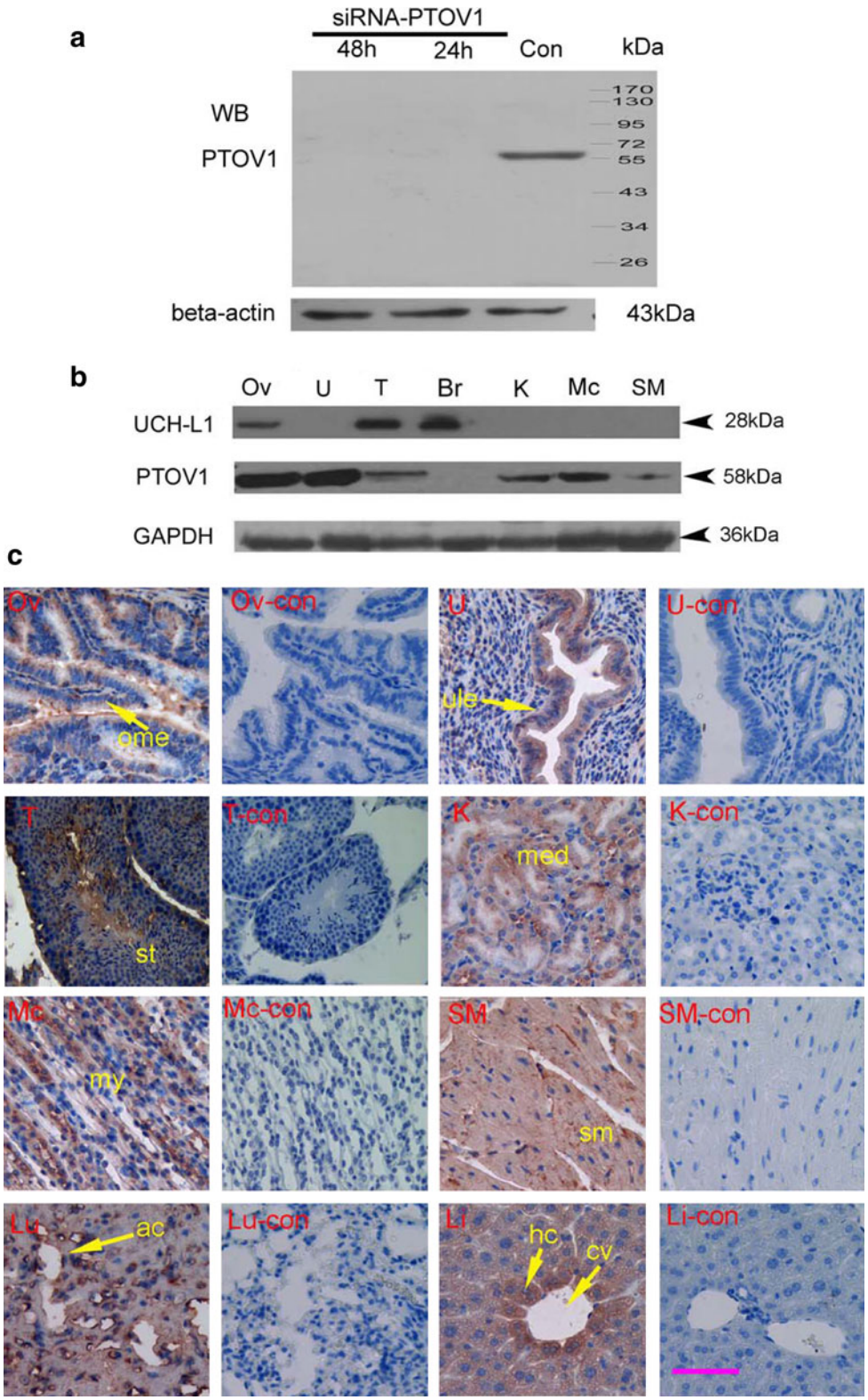

Fig. 2 Expression and subcellular localization of PTOV1 in various adult mouse tissues **a** Western blotting analysis with anti-PTOV1 antibodies on lysates from human A549 cells transfected with PTOV1 siRNA or control siRNA. And 24 and 48 h later, cells were harvested and processed for western blotting analysis as described in "Materials and methods". Beta-actin was used as an internal control. **b** Western blotting analysis with anti-PTOV1 and anti-UCH-L1 antibodies on adult mouse tissues. The following abbreviations are used: *Ov* ovary, *U* uterus, *T* testis, *Br* brain, *K* kidney, *Mc* myocardium, and *SM* skeletal muscle. GAPDH was used as a control for sample loading. **c** Immunohistochemical analysis of PTOV1 in adult mouse tissues. The panels show immunohistochemical results on sections of different adult mouse tissues including oviduct (*Ov*), uterus (*U*), testis (*T*), kidney (*K*), myocardium (*Mc*), skeletal muscle (*SM*), lung (*Lu*) and liver (*Li*), respectively. The Ov-con, U-con, T-con, K-con, Mc-con, SM-con, Lu-con and Li-con panels show the corresponding negative controls. *Yellow arrows* indicate the localization of PTOV1 in somatic cells. *ome* oviduct mucous epithelium, *ule* uterine luminal epithelium, *st* seminiferous tubule, *med* medulla of kidney, *my* myocytes, *sm* stritated muscle, *ac* alveolar cell of lung, *cv* central vein of the hepatic lobule, *hc* hepatocyte. *Pink bar* in the last panel marks 100 μm

the oocyte and the cytoplamic part near the oocyte of the innermost layer of granulosa cells (Fig. 3e, panel 2W). In 3, 4 and 8 week-old mouse ovaries, it was also abundant in the oocytes of secondary and tertiary follicles. In 4 week-old mouse, dendritic connections between the innermost layer of granulosa cells and oocyte plasma membrane occurred in some secondary follicles, and they could possibly consist of cell processes (Fig. 3e, panel 4W).

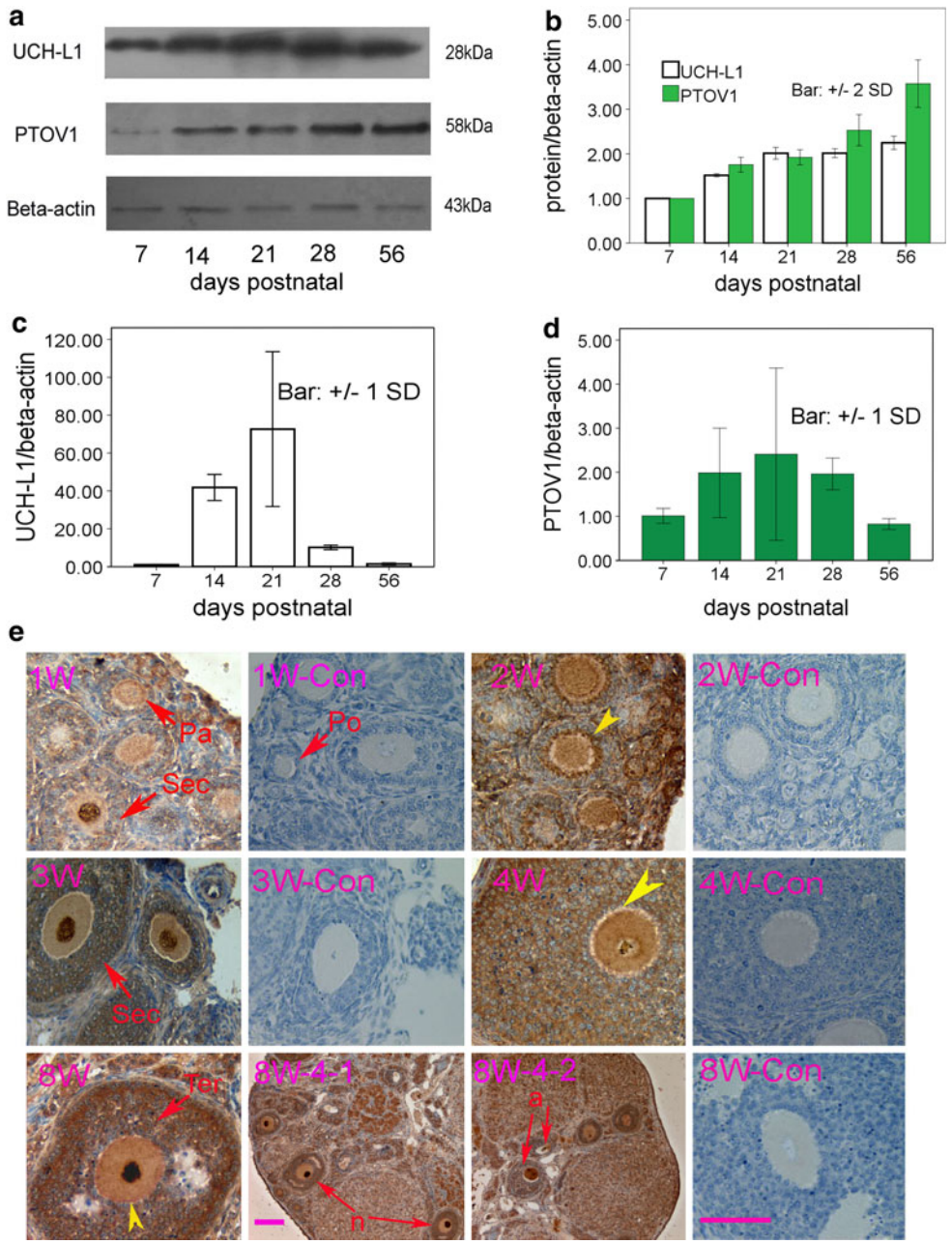

Fig. 3 Expression and subcellular localization of PTOV1 and UCH-L1 in mouse oocytes at different ages. **a** Western blot analysis of PTOV1 protein levels in mouse ovarian tissue protein extracts at different ages. **b** Quanatification by densitometric analysis of data in a. The data in **b**–**d** were all normalized to their corresponding data of day 7 postnatal. **c**, **d** mRNA levels of UCH-L1 and PTOV1 in mouse ovarian tissues at different ages. The mRNA levels were quantified by real-time RT-PCR with beta-actin gene as a reference. **e** Subcellular immunohistochemical characterization of PTOV1 in mouse oocytes at different ages. The panels 1W, 2W, 3W, 4W, and 8W show PTOV1 staining in mouse ovaries at the ages of 7, 14, 21, 28 and 56 days, respectively, and 8W-4-1 and 8W-4-2 are different observing fields of 8W ovarian sections. The panels 1W-Con, 2W-Con, 3W-Con, 4W-Con and 8W-Con show the corresponding negative controls. *Po* primordial follicles, *Pa* primary follicles, *Sec* secondary follicles, *Ter* tertiary follicles, as *red arrows* point. *Yellow arrowheads* in panel 2W indicate strong PTOV1 staining in the cytoplasm of granulosa cells around the oocyte in a primary follicle; and in panel 8W, *yellowheads* point to the strong PTOV1 staining in oocytes (panel 2W, 4W) and on the oocyte plasma membrane (panel 8W). In the two panels of 8W-4-1 and 8W-4-2, *n* oocytes of normal shapes, *a* oocytes of abnormal shapes. Panels 8W-4-1 and 8W-4-2 were amplified to 40×, and the rest panels to 100×. *Pink bar* in panel 8W-4-1 and the last panel marks 100 μm

Although PTOV1 was detected in the dendritic connections, it was morphologically different from the specific distribution of PTOV1 at the oocyte plasma membrane in secondary and tertiary follicles from 8-week-old mouse ovaries. For adult mice (56 d), strong PTOV1 expression was found in oocyte nuclei and its plasma membrane (Fig. 3e, panel 8W). Distribution of PTOV1 formed a specific ring structure around the oocyte plasma membrane, which was probably in relation to the dendritic connections found in 4-week-old mouse ovaries. In adult ovaries, some oocytes showed abnormal shapes (Fig. 3e, panel 8W-4-2), in which PTOV1 did not display the typical distribution patterns, or both in the nucleus and on the plasma membrane, as observed in Fig. 3e, Panels 8W and 8W-4-1. Weak or even no signals were found in the theca cells from prepuberty to sexual maturity. PTOV1 exclusively existed in the cytoplasm of granulosa cells as described above, even at different follicular development stages (Fig. 3e).

Estradiol affects the distribution and expression of PTOV1 in mouse ovaries

The above observations suggested that PTOV1 protein content in mouse ovaries varied from prepuberty to sexual maturity. The secretion of estrogen could increase with sexual development, so we determined whether the subcellular localization of PTOV1 in oocytes was affected by estrogen. We injected estradiol into the prepubertal mouse abdominal cavity to observe the possible actions of estradiol on PTOV1 localization by immunohistochemistry, and at the same time, on its expressional levels by Western blot analysis and RT-PCR analysis.

PTOV1 was densely distributed in oocyte nuclei and on plasma membranes in estradiol-treated prepubertal mouse ovaries (28 days postnatal), but no or weak PTOV1 staining was observed at oocyte plasma membranes in the control group. However, the distribution of PTOV1 in granulosa cells was not affected by estradiol (Fig. 4a). Moreover, the distribution of UCH-L1 in oocytes did not change similarly in response to estradiol stimuli (Fig. 4a).

In addition to the changes of PTOV1 distribution pattern in oocytes, the possible increase in its ovarian protein and mRNA levels caused by estradiol treatment in protein and mRNA levels of PTOV1 in the ovaries with estradiol treatment was studied. UCH-L1 and PTOV1 were similarly affected by estradiol. Only changes in protein levels were found statistically significant, as star marked in Fig. 4b, $p = 0.007$ for PTOV1 and $p = 0.034$ for UCH-L1. Although more or less, their corresponding mRNA levels had an increasing trends, but they did not reach a significant difference from Con group, $p = 0.278$ for PTOV1 and $p = 0.190$ for UCH-L1 as in Fig. 4c.

Discussion

The proteins isolated by immunoaffinity were identified by mass spectrometry, and it was found that PTOV1 was specifically bound to GST-UCH-L1 in adult mouse ovarian protein extracts. And GST panel, a negative control, did not show a specific band of PTOV1. Moreover, in the confirmation by WB, the specific band recognized by the PTOV1 antibody was presented. However, as reported by others (Benedit et al. 2001), its apparent molecular weight in SDS-PAGE is evaluated at 58 kDa, which is different from its theoretical molecular weight of 47 kDa. Otherwise, the results obtained by using siRNA interference and WB analysis on A549 cells also showed that our prepared antibody could specifically recognize the PTOV1 protein. So, according to the pull-down and WB results, we proposed that PTOV1 was specifically bound to UCH-L1, in vitro, even though this binding may be direct or indirect. However, their association in the oocytes could not be extrapolated to other tissues, for PTOV1 and UCH-L1 did not behave in the same way in tissue distribution specificity, for example in the brain, there is high expression of UCH-L1, but no expression of PTOV1 was detected.

PTOV1 can bind to flotillin-1 (Santamaria et al. 2005) and the 14-3-3 protein (Benzinger et al. 2005), which can interact with CDK1 (Chan et al. 1999). We have found that UCH-L1 is involved in toad oocyte maturation, and toad UCH-L1 is considered to specifically bind to CDK1 in toad oocyte protein extracts (Sun et al. 2002). So, in mouse oocytes UCH-L1 may be associated with the mitotic promoting factor (MPF), also known as maturation promoting factor, which consists of cyclin B1/B2 and CDK1 (or $p34^{cdc2}$). In present study, we demonstrated that there was an association between UCH-L1 and PTOV1, though we did not know whether a direct or indirect interaction existed between the two proteins in mouse. The interaction between UCH-L1 and CDK1 may be mediated by the action of PTOV1 and the 14-3-3 protein. The colocalization of PTOV1 and UCH-L1 in oocyte nuclei may be involved in regulating meiotic division. UCH-L1 is tightly associated with the mitotic spindle through all stages of M phase, suggesting that it plays an important role in microtubule formation (Bheda et al. 2010). Nuclear localization of PTOV1 is required for the stimulation of cell proliferation (Santamaria et al. 2005; Santamaria et al. 2003). PTOV1 is capable of CBP-binding, and CBP (CREB-binding protein) is first isolated as a nuclear protein that binds to cAMP-response element-binding protein (CREB) (Youn et al. 2010). In addition, CBP owns intrinsic histone acetyltransferase activity and can repress cyclin B2 expression and G_2/M transition (Wu et al. 2010). We found that PTOV1 occurred in the nuclei of oocytes, but in somatic cells of selected adult mouse tissues, it was

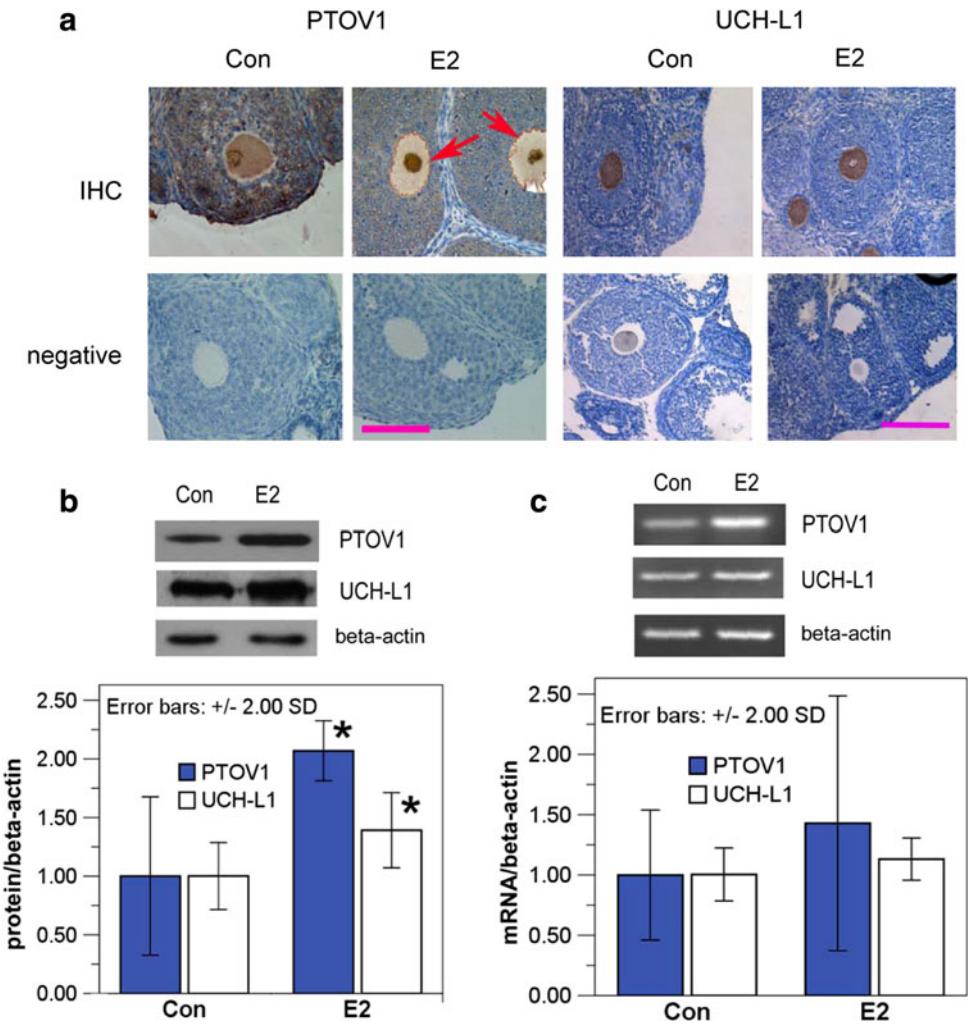

Fig. 4 Distribution of PTOV1 and UCH-L1 in oocytes and their expression in mouse ovaries with the estradiol treatment. **a** Localization of PTOV1 and UCH-L1 in estradiol-treated and control mouse ovaries. PTOV1-positive signal was intensified on the cytoplasmic membranes in estradiol-treated mouse oocytes (the *red arrows* pointed), and no such phenomenon was found in control mouse oocytes. UCH-L1 presented a similar distribution between the estradiol-treated mouse oocytes and control ones. *Pink bar* 100 μm. **b** Western blot analysis with anti-PTOV1 and anti-UCH-L1 antibodies on protein extracts from estradiol-treated and control mouse ovaries. **c** RT-PCR analysis of *PTOV1* and *UCH-L1* in estradiol-treated and control mouse ovaries. Data of the RNA and protein band intensity are presented as mean ± 2SD in panels **b** and **c**, and the data in **b** and **c** were both normalized to the corresponding Con. The *asterisks* in panel **b** indicate statistically significant difference from the corresponding control ($p < 0.05$)

present only in the cytoplasm. Its specific distribution pattern in oocytes indicated that PTOV1 played possible roles in the meiosis of oocytes, which were different from those in mitosis of somatic cells. Thus, PTOV1 and UCH-L1 may be associated with each other and specifically involved in the meiotic arrest at the G_2/M transition, but further investigations are required to clarify the related mechanisms in mouse oocyte development and maturation.

In this study, we found that protein levels of POTV1 and UCH-L1 in ovaries increased in parallel with mouse age, besides their binding with each other. But their mRNA levels did not show a similar increasing tendency. Both PTOV1 and UCH-L1 mRNA levels increased with age before 21 days postnatal, then turned to drop since 28 days postnatal. UCH-L1 hydrolytic activity can hydrolyze K48 ubiquitin chains to obtain ubiquitin monomers, which up-regulates the ubiquitination-dependent protein degradation; but when its concentration rises to a certain degree it can show ligase activity and promote the formation of K63 ubiquitin chain, which inhibits protein degradation in the proteasome and results in that the ubiquitinated proteins become more stable (Liu et al. 2002). The paralleled increases in the protein levels of PTOV1 and UCH-L1 with age may be due to the stabilization on PTOV1 caused by UCH-L1 at the high concentration in oocytes, or to other common factors affecting both of them in post-translation levels, even though it was not completely excluded the contribution from the changes in their mRNA levels with age.

And the unique distribution pattern of PTOV1 in oocytes was different from that in somatic cells. In mouse oocytes, the two proteins not only concentrated at the cytoplasmic membrane but also were aggregated in the nuclei in a similar pattern. In secondary and tertiary follicles of sexually mature mice ovaries, a ring-like structure at the oocyte plasma membrane was presented with strong specific PTOV1-positive signal, but it was not able to determine the source of the ring-like structure by immunohistochemistry. Probably, it was related to the PTOV1 strong staining in the cytoplasm of the innermost layer of granulosa cells in the primary follicles in 14-day-old mice, and it may come from the connections between the oocyte

and granulosa cells in secondary follicles in 28-day-old mice. This particular distribution of PTOV1 of the ring-like structure may be formed by both the oocyte plasma membrane and innermost cytoplasmic parts of granulosa cells, though further study is needed to determine the exact sources of its composition by means of the electron microscope. So, the specific distribution of PTOV1 proteins at occyte plasma membrane may be related to material exchange between oocytes and surrounding granulosa cells, which is pivotal for oocyte development and maturation. In the 56-day-old mouse ovaries, we found that some oocytes showed abnormal morphology and accompanied changes in the distribution of UCH-L1, so we supposed that UCH-L1 participated in the selective elimination of mouse oocytes (Gu et al. 2009). Similarly, the distribution pattern of PTOV1 has also paralleled abnormal changes. In mouse oocytes with abnormal shapes, no ring-like structure on the plasma membrane was observed. So, we speculate that PTOV1 may also be involved in the selective elimination in the process of mouse oocyte development.

Our results showed that exogenous estradiol promoted to form a specific PTOV1 distribution pattern in oocytes from the prepubertal mice, which suggested that PTOV1 was possibly transferred to the oocyte plasma membrane in response to the estrogen stimuli. A small amount of estradiol is produced in small antral follicles, and estradiol secretion levels increase to facilitate follicular development in large antral follicles and preovulatory follicles under the regulation of the hypothalamic-pituitary-ovary axis (Drummond 1999). In the process from birth to sexual maturity, UCH-L1 aggregated gradually towards the plasma membrane in mouse oocytes with the ovarian follicular development (Sekiguchi et al. 2006). However, whether its transfer coupled with UCH-L1 needed further study despite of their similar distribution pattern at the oocyte plasma membranes caused by estrodiol. Our results also showed that estradiol treatment can lead to that PTOV1 and UCH-L1 proteins in prepubertal mouse ovarian protein extracts were significantly increased, and otherwise mRNA levels did not change significantly. In the case that mRNA did not change significantly, the results on PTOV1 and UCH-L1 regulation at the protein level by estrogen will initiate further studies for many factors may be involved in the protein homostasis. UCH-L1 is required for toad oocyte maturation (Gu et al. 2009; Sun et al. 2002, 2003), but no data support that UCH-L1 is indispensable for oocyte maturation in mice. So it is difficult to understand how estrogen regulated oocyte development through PTOV1 and UCH-L1, but changes in distribution patterns of PTOV1 in mouse oocytes were in response to estrogen stimuli, and the association between PTOV1 and UCH-L1 reinforced the explication for their possible functions in oocyte meiotic arrest and maturation.

In summary, our results indicated that PTOV1 and UCH-L1 protein association occurred in mouse ovaries. The actions of PTOV1 and UCH-L1 on meiosis may be deduced from their relation to MPF. For PTOV1, similar to UCH-L1, a specific distribution pattern existed physiologically in adult mouse oocytes, though in oocytes with abnormal shapes, PTOV1 did not display the typical distribution patterns. PTOV1 was concentrated in the nucleus and at the plasma membrane in oocytes, which was different from the case in somatic cells. Exogenous estradiol promotes to form the specific distribution pattern of PTOV1, not of UCH-L1, in prepubertal mouse oocytes. The specific distribution of PTOV1 protein, which was found on the plasma membrane in adult mouse oocytes, was probably derived from the morphological manifestation of high PTOV1 expression in connections between oocyte and granulosa cells in prepubertal mouse ovaries.

Acknowledgments We thank the National Natural Science Foundation of China (#30672247) and National Basic Research Program of China (2006CB504005) for financial support.

References

Benedit P, Paciucci R, Thomson TM, Valeri M, Nadal M, Caceres C, de Torres I, Estivill X, Lozano JJ, Morote J, Reventos J (2001) PTOV1, a novel protein overexpressed in prostate cancer containing a new class of protein homology blocks. Oncogene 20:1455–1464

Benzinger A, Muster N, Koch HB, Yates JR 3rd, Hermeking H (2005) Targeted proteomic analysis of 14-3-3 sigma, a p53 effector commonly silenced in cancer. Mol Cell Proteomics 4:785–795

Bheda A, Gullapalli A, Caplow M, Pagano JS, Shackelford J (2010) Ubiquitin editing enzyme UCH L1 and microtubule dynamics: implication in mitosis. Cell Cycle 9:980–994

Bristol-Gould SK, Kreeger PK, Selkirk CG, Kilen SM, Cook RW, Kipp JL, Shea LD, Mayo KE, Woodruff TK (2006) Postnatal regulation of germ cells by activin: the establishment of the initial follicle pool. Dev Biol 298:132–148

Chan TA, Hermeking H, Lengauer C, Kinzler KW, Vogelstein B (1999) 14-3-3 Sigma is required to prevent mitotic catastrophe after DNA damage. Nature 401:616–620

De Felici M, Klinger FG, Farini D, Scaldaferri ML, Iona S, Lobascio M (2005) Establishment of oocyte population in the fetal ovary: primordial germ cell proliferation and oocyte programmed cell death. Reprod Biomed Online 10:182–191

Drummond AE, Findlay JK (1999) The role of estrogen in folliculogenesis. Mol Cell Endocrinol 151:57–64

Gu YQ, Chen QJ, Gu Z, Shi Y, Yao YW, Wang J, Sun ZG, Tso JK (2009) Ubiquitin carboxyl-terminal hydrolase L1 contributes to the oocyte selective elimination in prepubertal mouse ovaries. Sheng Li Xue Bao 61:175–184

Hutt KJ, Albertini DF (2007) An oocentric view of folliculogenesis and embryogenesis. Reprod Biomed Online 14:758–764

Liu Y, Fallon L, Lashuel HA, Liu Z, Lansbury PT Jr (2002) The UCH-L1 gene encodes two opposing enzymatic activities that affect alpha-synuclein degradation and Parkinson's disease susceptibility. Cell 111:209–218

Livak KJ, Schmittgen TD (2001) Analysis of relative gene expression data using real-time quantitative PCR and the 2(-Delta Delta C(T)) Method. Methods (San Diego, Calif) 25:402–408

Miyano T, Manabe N (2007) Oocyte growth and acquisition of meiotic competence. Soc Reprod Fertil Suppl 63:531–538

Morote J, Fernandez S, Alana L, Iglesias C, Planas J, Reventos J, Ramon YCS, Paciucci R, de Torres IM (2008) PTOV1 expression predicts prostate cancer in men with isolated high-grade prostatic intraepithelial neoplasia in needle biopsy. Clin Cancer Res 14:2617–2622

Nakamura Y, Suzuki T, Igarashi K, Kanno J, Furukawa T, Tazawa C, Fujishima F, Miura I, Ando T, Moriyama N, Moriya T, Saito H, Yamada S, Sasano H (2006) PTOV1: a novel testosterone-induced atherogenic gene in human aorta. J Pathol 209:522–531

Piccinini M, Merighi A, Bruno R, Cascio P, Curto M, Mioletti S, Ceruti C, Rinaudo MT (1996) Affinity purification and characterization of protein gene product 9.5 (PGP9.5) from retina. Biochem J 318:711–716

Plancha CE, Sanfins A, Rodrigues P, Albertini D (2005) Cell polarity during folliculogenesis and oogenesis. Reprod Biomed Online 10:478–484

Rosenfeld CS, Wagner JS, Roberts RM, Lubahn DB (2001) Intraovarian actions of oestrogen. Reproduction 122:215–226

Sakai N, Sawada MT, Sawada H (2004) Non-traditional roles of ubiquitin-proteasome system in fertilization and gametogenesis. Int J Biochem Cell Biol 36:776–784

Santamaria A, Castellanos E, Gomez V, Benedit P, Renau-Piqueras J, Morote J, Reventos J, Thomson TM, Paciucci R (2005) PTOV1 enables the nuclear translocation and mitogenic activity of flotillin-1, a major protein of lipid rafts. Mol Cell Biol 25:1900–1911

Santamaria A, Fernandez PL, Farre X, Benedit P, Reventos J, Morote J, Paciucci R, Thomson TM (2003) PTOV-1, a novel protein overexpressed in prostate cancer, shuttles between the cytoplasm and the nucleus and promotes entry into the S phase of the cell division cycle. Am J Pathol 162:897–905

Sato E, Kimura N, Yokoo M, Miyake Y, Ikeda JE (2006) Morphodynamics of ovarian follicles during oogenesis in mice. Microsc Res Tech 69:427–435

Sekiguchi S, Kwon J, Yoshida E, Hamasaki H, Ichinose S, Hideshima M, Kuraoka M, Takahashi A, Ishii Y, Kyuwa S, Wada K, Yoshikawa Y (2006) Localization of ubiquitin C-terminal hydrolase L1 in mouse ova and its function in the plasma membrane to block polyspermy. Am J Pathol 169:1722–1729

Song JL, Wessel GM (2005) How to make an egg: transcriptional regulation in oocytes. Differentiation 73:1–17

Sun ZG, Kong WH, Yan S, Gu Z, Zuo JK (2003) The functions in the progesterone-induced oocyte maturation of toad ubiquitin carboxyl-terminal hydrolase (tUCH) is independent of its UCH activity. Shi Yan Sheng Wu Xue Bao 36:105–112

Sun ZG, Kong WH, Zhang YJ, Yan S, Lu JN, Gu Z, Lin F, Tso JK (2002) A novel ubiquitin carboxyl terminal hydrolase is involved in toad oocyte maturation. Cell Res 12:199–206

Wilkinson KD, Cox MJ, Mayer AN, Frey T (1986) Synthesis and characterization of ubiquitin ethyl ester, a new substrate for ubiquitin carboxyl-terminal hydrolase. Biochemistry 25:6644–6649

Wu T, Zhang X, Huang X, Yang Y, Hua X (2010) Regulation of cyclin B2 expression and cell cycle G2/m transition by menin. J Biol Chem 285:18291–18300

Youn HS, Park UH, Kim EJ, Um SJ (2010) PTOV1 antagonizes MED25 in RAR transcriptional activation. Biochem Biophys Res Commun 404:239–244